# Ignition and Extinction in the Catalytic Oxidation of Hydrocarbons over Platinum

**Götz Veser and Lanny D. Schmidt**
Dept. of Chemical Engineering and Materials Science, University of Minnesota, Minneapolis, MN 55455

*The ignition–extinction behavior in the oxidation of methane, ethane, propane and isobutane, as well as of ethylene and propylene over a platinum-foil catalyst was studied over the entire range of fuel/air ratios at atmospheric pressure. Ignition and extinction of the heterogeneous surface reaction, homogeneous ignition and the autothermal behavior of these fuel–air mixtures were investigated. The results show a common trend in the ignition extinction behavior of the alkanes and a different trend for the olefins. This is discussed in terms of a simple model, which correctly predicts the composition dependence of the surface ignition curve for reasonable values of parameters, indicating a mainly oxygen-covered surface during ignition of the alkanes and a mainly hydrocarbon-covered surface in the case of the olefins. Different branches of the complete bifurcation diagrams are discussed separately, allowing qualitative conclusions about the catalytic activity of Pt for the oxidation reactions of different fuels.*

## Introduction

The ignition–extinction behavior of catalytic reactions has both scientific and applied interest. It is crucial for the understanding of catalytic surface reactions such as catalytic partial oxidation of hydrocarbons (Germain, 1969; Satterfield, 1991; Trimm, 1983), as well as for the total oxidation of fossil fuels in catalytically stabilized burners (Pfefferle and Pfefferle, 1987). Also, in the ignition of homogeneous gas-phase combustion, the ignition at hot catalytic or noncatalytic surfaces remains an important and still poorly understood phenomenon (Frank-Kamenetskii, 1969; Liñán and Williams, 1993). In this context, the coupling between heterogeneous surface reaction and homogeneous gas-phase reactions at high temperatures has recently received considerable interest, since this coupling can strongly influence the selectivity of industrial catalytic processes (Cattolica and Schefer, 1982; Lunsford, 1989; Thomas et al., 1992). An additional concern in the oxidation of hydrocarbons is process safety since hydrocarbon/air mixtures tend to be highly flammable and explosive over a wide range of compositions. It is therefore crucial to understand their ignition–extinction behavior under realistic conditions (Lewis and von Elbe, 1987). Yet, under these conditions, the surface coverages usually become too low to be detectable with the standard UHV techniques, so that these reaction systems are typically not amenable to detailed mechanistic studies.

While many studies have been conducted to elucidate some of the mentioned problems, most of these studies were only concerned with specific points of these questions (Ablow et al., 1980; Cho and Law, 1986; Coward and Guest, 1927; Griffin et al., 1989; Harold and Luss, 1985, 1987; Harold et al., 1987, Hiam et al., 1968; Patterson and Kemball, 1963; Schwartz et al., 1971). Since experimental configurations and conditions of those investigations differ widely, a comparable set of data for different fuels over a range of different conditions such as compositions and/or temperatures cannot be found in the published literature. The present investigation tries to close this gap by establishing complete bifurcation diagrams for the homogeneous and heterogeneous ignition–extinction behavior of different fuels using a single well-defined experiment for six different hydrocarbons.

## Experimental Studies

The experiments were all conducted in a glass flow tube of 2.5-cm diameter and 20-cm length. Gases were introduced through mass flow controllers and premixed in a premixing zone filled with glass beads. The $15 \times 5 \times 0.025\text{-mm}^3$ catalytic Pt foil (Johnson Matthey, 99.99% purity) was placed perpendicular to the gas flow in a stagnation flow configuration (Figure 1a). The foil was resistively heated, and by measuring

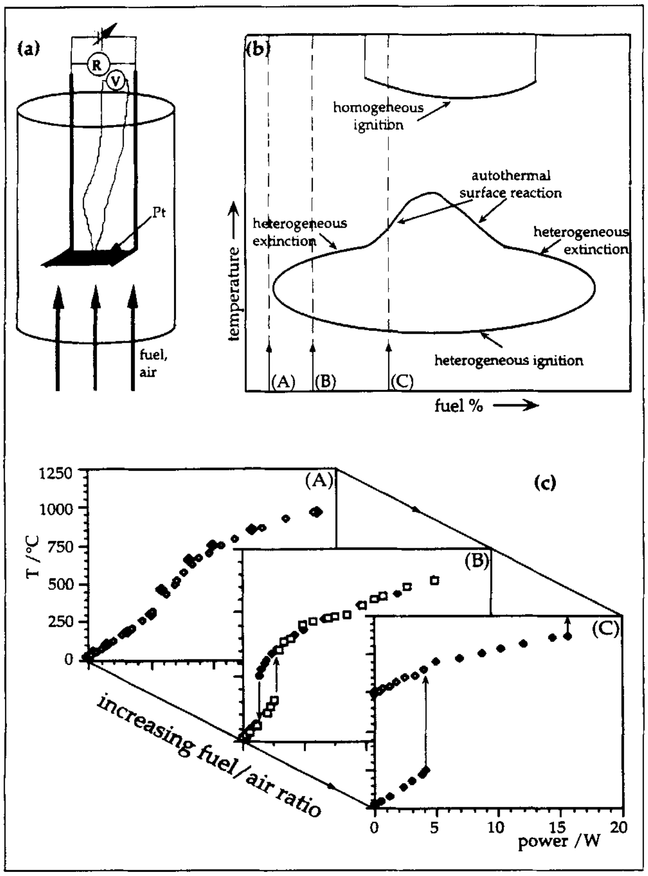

**Figure 1. (a)Experiment; (b) typical bifurcation diagram, indicating the branches for surface ignition and extinction, autothermal behavior, and homogeneous gas-phase ignition; (c) typical experimental S-curves for (A) transition from unreactive to reactive behavior, (B) hysteresis with ignition and extinction of the surface reaction, and (C) hysteresis with ignition and nonextinguishable, autothermal surface reaction as well as homogeneous ignition.**

The example given is for 1%, 2%, and 3% isobutane in 3 slpm air. The corresponding cuts are indicated by the dashed lines in the bifurcation diagram in Figure 1b.

the current output of the power supply and the voltage drop across the foil, the power input into the foil was determined. The foil temperature was measured via a chromel/alumel thermocouple spot-welded to the back of the foil. All experiments were conducted at a constant air flow rate of 3 slpm (velocity of ≈ 2.5 cm/s). Depending on the particular experimental conditions (fuel, fuel:air ratio, temperature) Reynolds numbers *Re* varied between 1 and 200, while Nusselt numbers *Nu* were between 30 and 500. Varying the total flow rate of the gases between 1 slpm and 6 slpm did not affect the results within experimental error in that ignition temperatures were unchanged to within ±20 K.

In a typical experiment, the power input was varied at a fixed fuel/air ratio, and the ignition and extinction temperatures of the heterogeneous reaction were determined from the power–temperature trace as turning points (i.e., saddle–node bifurcations) of the resulting hysteresis curves (Figure 1b, 1c). Thus, surface ignition is defined in our experiments by the occurrence of a temperature hysteresis, since this is a well-defined point in any experiment, as opposed to the observation of heat evolved due to the surface reaction (which is usually negligible before the occurrence of a hysteresis).

In the case of nonextinguishable mixtures, the foil temperature at zero power input (after ignition of the surface reaction) is taken as the autothermal temperature. Homogeneous ignition, or ignition of the noncatalytic gas phase reaction, was defined by the occurrence of a visual flame in the reactor. For safety reasons, the fuel supply was immediately shut off after the occurrence of homogeneous ignition. In this case, it was usually not possible to determine ignition and extinction points in a single run. Instead, ignition–extinction behavior of the heterogeneous reaction and homogeneous ignition were determined in separate consecutive runs. This procedure was repeated with different fuel/air ratios until the entire bifurcation diagram was completed, that is, until both the fuel-lean and fuel-rich limits of the surface flammability of the fuel were reached.

Data acquisition as well as control of the power input during an experiment were computer controlled using an Apple Macintosh-based data-acquisition system. A data point was defined as "stationary" when the mean value (taken over 10 s) of both the power input (the product of current input and voltage drop across the foil) and the catalyst temperature did not vary by more than twice the noise level over a period of one minute. For each fuel, the experiments were run with at least two different foils, and each branch of the bifurcation diagram was reproduced at least once. The data were reproducible between independent runs with different catalyst foils within ±50 K accuracy, while independent runs on the same catalyst foil were typically reproducible within ±20 K error.

The data were then plotted in a bifurcation diagram, which depicted the ignition and extinction temperatures of the heterogeneous reaction (or autothermal temperatures for nonextinguishable mixtures) as well as the ignition temperature of the homogeneous (gas-phase) reaction vs. a corrected equivalence ratio Θ (Williams et al., 1991). The latter is defined based on the usual equivalence ratio Φ:

$$\Phi = \frac{(\%\ \text{fuel}/\%\ \text{air})}{(\%\ \text{fuel}/\%\ \text{air})_{\text{stoich.}}}$$

which maps the fuel/air ratios independent of the specific nature of the fuel onto a scale of 0 to 1 for fuel-lean and 1 to infinity for fuel-rich mixtures. To put equal weight on both the fuel-lean and fuel-rich sides of the diagram (i.e., to make the diagram symmetric around the stoichiometric point for total oxidation), we transform this onto an axis by defining the corrected equivalence ratio Θ as

$$\Theta = \frac{\Phi}{1+\Phi}.$$

On this axis, the stoichiometric ratio for total oxidation to $CO_2$ and $H_2O$ is $\Theta = 0.5$, with the fuel-lean mixtures extending from 0 to 0.5 and the fuel-rich ones from 0.5 to 1. This corrected equivalence ratio will be used throughout this article and will furthermore be simply referred to as "equivalence ratio."

After ignition of the surface reaction, the hydrocarbons undergo total (I) and partial oxidation reactions II–IV, which are listed here for ethane:

$$\text{(I)}\quad C_2H_6 + 3.5O_2 \leftarrow, \rightarrow 2CO_2 + 3H_2O \quad (\Theta = 0.5)$$

$$\text{(II)}\quad C_2H_6 + 2.5O_2 \leftarrow, \rightarrow 2CO + 3H_2O \quad (\Theta = 0.58)$$

$$\text{(III)}\quad C_2H_6 + O_2 \leftarrow, \rightarrow 2CO + 3H_2 \quad (\Theta = 0.78)$$

$$\text{(IV)}\quad C_2H_6 + 0.5O_2 \leftarrow, \rightarrow C_2H_4 + H_2O \quad (\Theta = 0.88)$$

The (corrected) equivalence ratio at the stoichiometric point for the corresponding reaction is given in parentheses. Except for the equivalence ratio for total oxidation, which by definition is 0.5 for any fuel, these values will be slightly different for different fuels due to changes in the stoichiometries of the oxidation reactions. Obviously, the chemistry changes with increasing equivalence ratio from complete combustion (I), which dominates for any fuel-lean mixture up to $\Theta = 0.5$, toward the formation of more valuable oxidation products such as synthesis gas (III) and oxidative dehydrogenation to the corresponding olefin (IV). Thus, while catalytic combustors are typically run under very fuel-lean conditions ($\Theta \ll 0.5$), the interesting chemistry for partial oxidation reactions occurs on the fuel-rich side of the bifurcation diagram ($0.5 < \Theta < 1$).

## Results

### *Alkanes*

Figure 2 summarizes in four bifurcation diagrams the many experimental S-curves for ignition, extinction, and autothermal behavior of the four alkanes studied in this investigation. For each branch, only a couple of the experimental data points are given along with the corresponding interpolated curves.

It is obvious that the qualitative behavior of these four fuels is very similar. All four alkanes show a comparable range of surface flammability, which includes a region of autothermal behavior (i.e., nonextinguishable surface reaction) centered around a peak temperature at $\Theta \approx 0.6$. All homogeneous flammability limits lie between equivalence ratios of about 0.35 and 0.7. For comparison between the different fuels, the different branches of the bifurcation diagram will be shown and described in separate graphs in the following figures.

### *Surface ignition*

The surface ignition temperatures for the four alkanes vs. equivalence ratio are shown in Figure 3. For all four alkanes the region of surface flammability extends from an equivalence ratio of about 0.25 to about 0.9 (Table 1). At any fixed equivalence ratio, the ignition temperature drops with increasing carbon number from methane to ethane and propane, while it is virtually indistinguishable between propane and butane. This trend is somewhat less pronounced for fuel-rich mixtures due to the slight increase in ignition temperature for the C2–C4 alkanes toward the high-Θ end of the surface-ignition curves.

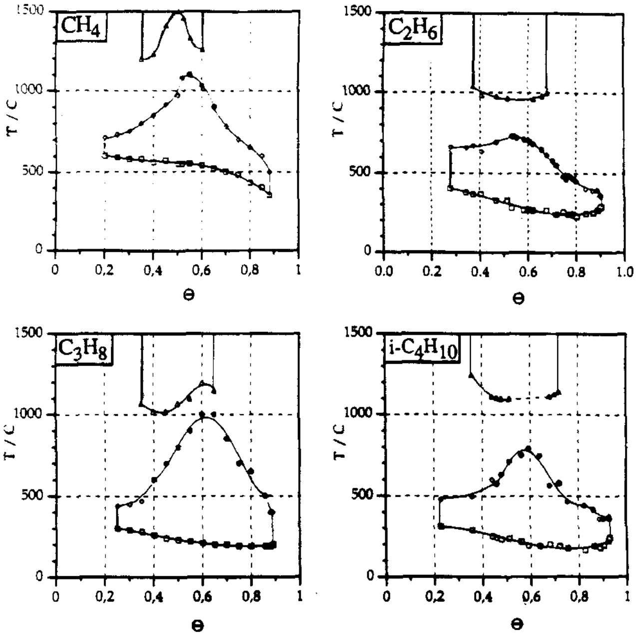

**Figure 2. Complete bifurcation diagrams for the four alkanes studied in this investigation.**

The diagrams were all obtained from S-curves of ignition and extinction, with the data being reproduced on several Pt foils.

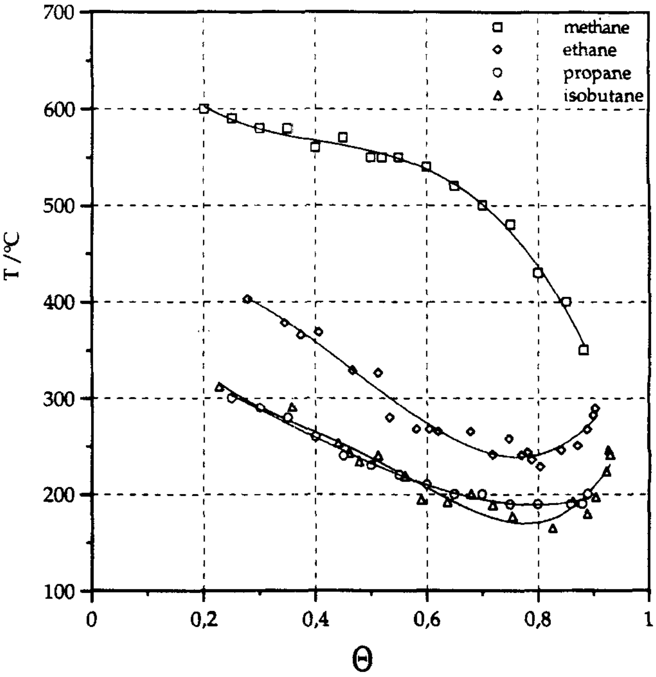

**Figure 3. Surface ignition branches for the four alkanes.**

Depicted is the ignition temperature of the heterogeneous surface reaction vs. equivalence ratio Θ.

For each alkane, the ignition temperature *decreases* with increasing fuel/air ratio. Yet, while the ignition temperatures run roughly parallel on the fuel-lean side of the bifurcation diagrams for all four alkanes, the behavior changes on the

**Table 1. Limits of Surface Flammability for Different Saturated and Unsaturated Hydrocarbons Studied in this Investigation***

| Fuel | $\Theta_1$ | $T_1$/°C | $\Theta_2$ | $T_2$/°C |
|---|---|---|---|---|
| Methane | 0.20 | 650 | 0.88 | 425 |
| Ethane | 0.27 | 525 | 0.90 | 325 |
| Propane | 0.25 | 350 | 0.90 | 300 |
| Isobutane | 0.22 | 400 | 0.93 | 300 |
| Ethylene | 0.11 | 460 | — | — |
| Propylene | 0.11 | 480 | — | — |

*$\Theta_1$, $\Theta_2$ denote the equivalence ratios at the fuel lean and fuel rich ends of the region of surface flammability, $T_1$ and $T_2$ the corresponding temperatures.

fuel-rich side. The C2–C4 alkanes show a minimum ignition temperature at an equivalence ratio of about 0.82, which then increases toward the fuel-rich end of the ignition branch, while the ignition temperature for methane keeps falling over the whole range of surface flammability.

### *Surface extinction and autothermal behavior*

The branches for the extinction of the surface reaction do not contain much additional information and are not depicted separately. For all four fuels they fall into a fuel-lean and a fuel-rich portion, separated by a region of autothermal behavior of the surface reaction. These autothermal branches of the bifurcation diagrams are shown in Figure 4. All four curves display a maximum temperature at an equivalence ratio of ~ 0.6, and with the exception of methane, extend from $\Theta \approx 0.45$ to about 0.8. The autothermal range for methane/air mixtures is considerably narrower, extending only from $\Theta \sim 0.52$ to about 0.65. Unlike the ignition and extinction temperatures, the autothermal temperatures do not show a uniform trend with increasing carbon number. Instead, the autothermal temperatures of methane and propane, on the one hand, and those of ethane and isobutane, on the other hand, lie close together.

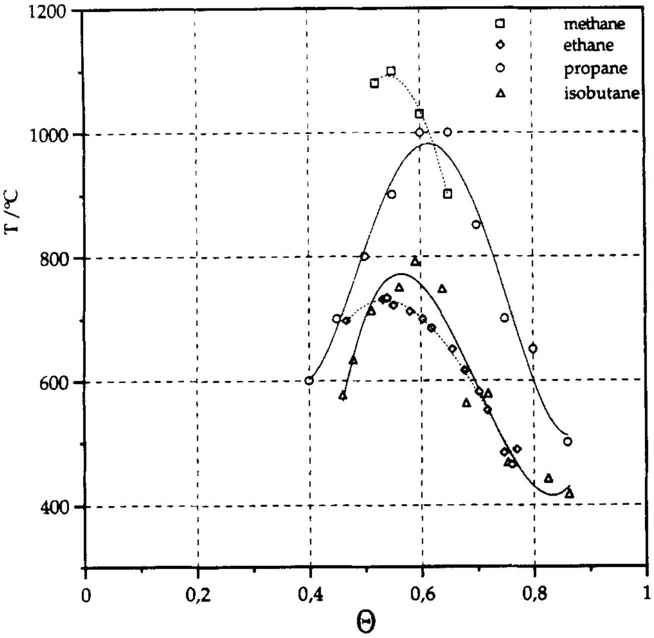

**Figure 4. Autothermal branches for the four alkanes.**

Depicted is the temperature of the catalyst foil after igniting the surface reaction and then turning off the external power supply vs. equivalence ratio Θ.

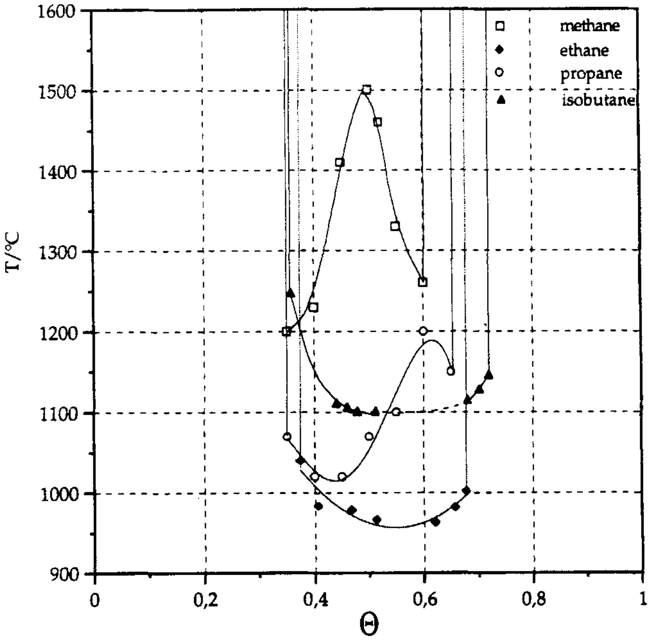

**Figure 5. Homogeneous ignition temperatures for the four alkanes.**

Depicted is the temperature of the catalyst foil immediately before observing a visible flame in the reactor vs. the modified equivalence ratio Θ.

### *Homogeneous ignition*

Finally, the homogeneous ignition temperatures for the four alkanes are shown in Figure 5. Again, the picture is somewhat disparate. For all four alkanes the lower flammability limit lies close to $\Theta \sim 0.35$. The higher limits vary from fuel to fuel, showing a general trend toward higher values with higher carbon numbers. The dependence of the ignition temperature on the fuel/air ratio shows no common trend for the different fuels. While the methane data display a distinct maximum at the stoichiometric mixture for total oxidation, the ethane and isobutane data indicate a flat minimum around that point, while the temperatures for the propane/air mixtures run through a minimum at $\Theta \sim 0.4$ and reach a maximum at $\Theta \sim 0.6$. (The lack of data points for isobutane between $\Theta \sim 0.5$ and 0.7 is due to the fact that the explosions at homogeneous ignition while approaching this region became so violent that the experiments were stopped before reaching the gas-phase ignition for these equivalence ratios.) The ignition temperatures for the C2–C4 alkanes lie between 950° and 1,250°C, while methane/air mixtures ignite at about 300°C higher temperatures, peaking at $T = 1{,}500$°C.

### *Olefins*

The experiments were extended to include olefins to allow a comparison between the behavior of saturated and unsaturated hydrocarbons over a Pt catalyst. The corresponding ex-

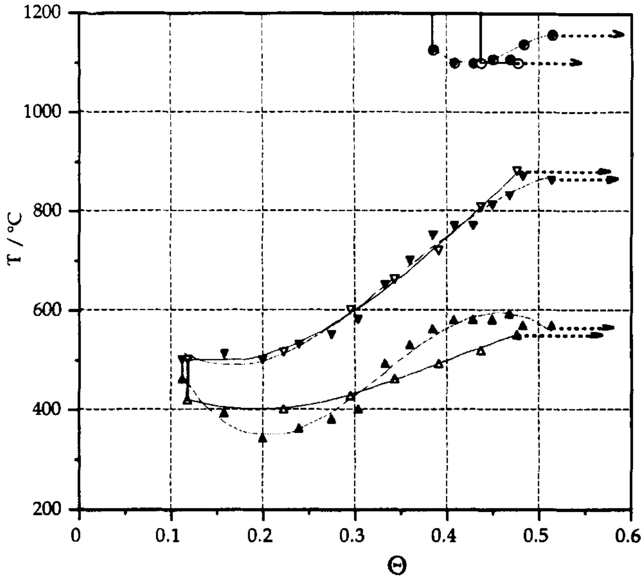

**Figure 6. Fuel-lean part of the bifurcation diagrams for ethylene (open symbols) and propylene (close symbols).**

Depicted are the surface ignition temperatures (upright triangles), surface extinction temperatures (downward triangles), and the homogeneous ignition temperatures (circles) vs. equivalence ratio Θ.

perimental bifurcation diagrams are shown in Figure 6. As one can clearly see, the two olefins are virtually indistinguishable in their surface ignition–extinction behavior as well as their homogeneous ignition behavior. The surface flammability of both fuels extends down to an equivalence ratio of about 0.11, that is, well below the fuel-lean limit for the alkanes. From there, the surface ignition temperature runs through a flat minimum at $\Theta \sim 0.2$ with increasing fuel content, and then rises to a maximum around the stoichiometric composition for total oxidation. The extinction temperatures follow that curve closely. The homogeneous ignition data for propylene extend to somewhat leaner mixtures ($\Theta \sim 0.39$) than those for ethylene ($\Theta \sim 0.44$). No autothermal behavior was found for these fuels within the range of fuel/air ratios that were studied. Both ignition and extinction of the olefins occur at considerably higher temperatures as compared to the C2–C3 alkanes.

We did not take any data points beyond an equivalence ratio of $\Theta \sim 0.5$ for either olefin, since the fuel-rich olefin/air mixtures reacted explosively upon homogeneous ignition of the gas phase. Since the foil temperature upon heterogeneous ignition of the surface reaction was increasing to within a few degrees of the homogeneous ignition temperatures, we also decided not to continue the surface ignition–extinction part of the bifurcation diagram out of safety concerns. Also, an alternative approach from the fuel-rich side of the bifurcation diagram turned out not to be of any help, since under fuel-rich conditions no surface ignition could be detected up to catalyst temperatures of 1,000°C.

In summarizing experiments, we stress again the surprisingly good reproducibility of the data for all equivalence ratios. Even on the very fuel-rich side of the bifurcation diagram, where heavy coking of the catalyst is predicted by thermodynamics and therefore should strongly limit the reproducibility of the experimental results, all measured temperatures were well reproducible within no more than ±20 K error between independent runs with the same Pt foil and no more than ±50 K error between runs with different catalyst foils. Also, we did not notice any dependency of the data on the "history" of the catalyst foil, that is, the data points of the bifurcation diagram could be recorded in any sequence without changes in the results.

## Discussion

The most obvious result of this investigation for the catalytic combustion of hydrocarbons is the observation that there is no break or noticeable qualitative change in the bifurcation diagram of any hydrocarbon while crossing from the fuel-lean to the fuel-rich side of the diagrams. Obviously, the stoichiometric ratio for total oxidation ($\Theta = 0.5$) does not have any specific importance for the ignition–extinction behavior of the surface reactions. Instead, the ignition curves can be explained by catalytic site competition between the fuel and oxygen on the Pt surface. The curve for alkanes can be explained in terms of a mainly oxygen-covered surface, while the ignition curve for the olefins indicates the presence of a carbon-containing layer on the catalyst.

We will discuss this and other results separately in more detail in the following subsection.

### *Surface ignition*

The surface-ignition branch of the bifurcation diagram is probably the most important and most interesting part of the experimental results. Ignition of the surface reaction is obviously an essential requirement in any catalytic process. A high ignition temperature will require a high degree of external preheating of the catalytic reactor or the addition of another more easily ignitable fuel during the startup procedure, both of which add to the overall cost of the process and create safety hazards. It is therefore essential to have a good knowledge of ignition temperatures and their dependence on the fuel/air ratio. Additionally, the dependence of the ignition temperature on the equivalence ratio can also provide valuable information for a mechanistic understanding of the surface reaction during ignition, as will be seen below.

The surface-ignition temperatures of the alkane/air mixtures are characterized by two obvious qualitative trends: the ignition temperatures decrease with (1) increasing carbon number, and (2) increasing fuel content of the gas mixture. The drop in ignition temperature with increasing carbon number can be expected, since the activation of the alkane on the catalyst surface is known to follow the C—H bond strength of the hydrocarbons (McMaster et al., 1993; McMaster and Madix, 1993; Szuromi et al., 1985). This is shown in Figure 7, which depicts the ignition temperatures for the alkanes at various equivalence ratios vs. the bond strength of the weakest C—H bond for three different equivalence ratios (Benson, 1965). As expected, the ignition temperature increases with increasing C—H bond energy, though there is not a simple linear dependence between the two quantities, indicating that the C—H bond strength is not the only factor determining the observed behavior. Obviously, other factors such as differences in the sticking coefficient between the hy-

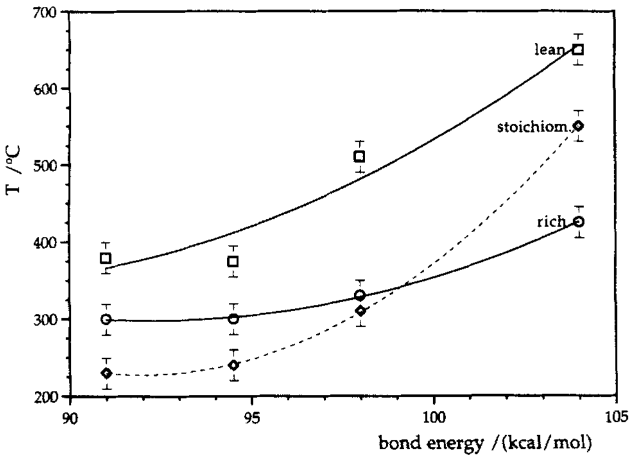

**Figure 7. Ignition temperatures for the four alkanes vs. corresponding bond strength (Benson, 1965).**

The ignition temperatures given are for the lean (squares) and rich (circles) limits of the hydrocarbon/air mixtures as well as the stoichiometric composition (diamonds) for total oxidation ($\Theta = 0.5$).

drocarbons will also have to be taken into account for a more realistic description of the systems as will be shown further below.

Another interesting point that becomes apparent from this plot is the fact that methane behaves qualitatively differently from the higher hydrocarbons in so far as the ignition temperature does not show a local minimum anywhere in the fuel-rich part of the bifurcation diagram. This causes the crossing of the curves for the stoichiometric and the fuel-rich mixtures in the plot. This behavior can be explained by an increasing (dissociative) sticking coefficient with increasing carbon number: A higher fuel sticking coefficient causes a poisoning of the catalyst surface at lower fuel/air ratios. Therefore, the decreasing trend in ignition temperatures will terminate at lower fuel/air ratios, causing the curve of the ignition temperatures $T(\Theta)$ to bend upward (i.e., toward higher $T$). Such an increasing trend in sticking coefficients with increasing carbon number was indeed observed by McMaster et al. in molecular-beam experiments with different hydrocarbons over a Pt(111) single crystal (McMaster et al., 1993). Although the experiments were conducted under very different conditions [UHV, clean Pt(111) surface, low temperature, etc.], and therefore are certainly not directly comparable to our experimental conditions, it seems nevertheless reasonable to assume a qualitatively similar trend. In particular, this also helps to explain the stronger than linear dependence of ignition temperature on the C—H bond strength, since the sticking coefficient follows the same trend vs. carbon number as does the bond strength. Finally, the fact that the sticking coefficient as measured by McMaster and Madix (1993) shows a marked increase from methane to ethane, but only a slight increase from ethane to propane, fits well into this picture, since it correlates with both the sharp decrease in ignition temperature from methane to ethane in our data and the fact that only the methane/air mixtures do not display a minimum ignition temperature within the range of surface flammabilities.

Despite the lack of data for sticking coefficients of olefins on clean or oxygen-covered Pt surfaces, it is tempting to extend the preceding reasoning to explain the markedly different qualitative behavior of the ignition temperatures of the olefins vs. equivalence ratio. These opposite trends in ignition temperatures for olefins and alkanes have been observed by Cho and Law, although these authors only studied a comparatively narrow range of fuel/air ratios in the fuel-lean regime (Cho and Law, 1986). They tentatively explained their observation by the different "adsorption strength" (i.e., sticking coefficients) of the hydrocarbons against oxygen.

### *A simple model: Alkanes*

To test these hypotheses, we set up a simplified model that balances conductive heat losses (neglecting radiative heat losses due to the comparatively low catalyst temperatures up to surface ignition) and heating of the catalyst surface through the external resistive heating as well as the heat evolved by the surface reaction itself. The heat balance of the system is thus

$$\alpha(T - T_0) = VI + r\Delta H_R, \tag{1}$$

where $\alpha$ denotes the heat transfer coefficient (for simplicity, lumped with the surface area of the catalytic foil), $(VI)$ is the external power input through the resistive heating, and $r\Delta H_R$ is the heat evolved due to the surface reaction.

Furthermore we assume for the surface reaction a simple, first-order Langmuir–Hinshelwood (LH) mechanism with competitive, nondissociative adsorption of the reactant gases:

$$\mathrm{HC} + \mathrm{S} \leftarrow, \rightarrow \mathrm{HC{-}S} \qquad \text{(RI)}$$

$$\mathrm{O_2} + \mathrm{S} \leftarrow, \rightarrow \mathrm{O_2{-}S} \qquad \text{(RI)}$$

$$\mathrm{HC{-}S} + \mathrm{O_2{-}S} \rightarrow 2\mathrm{S} + \text{products}, \qquad \text{(RIII)}$$

where $HC$ denotes the respective hydrocarbon, and S denotes an active site on the catalyst surface. Obviously, both the assumption of the surface reaction being first order in oxygen and the hydrocarbon, as well as the assumption of nondissociative adsorption, are gross simplifications. On the one hand, dissociative adsorption is, at least for oxygen adsorption on platinum, well established by now, while, on the other hand, the detailed surface chemistry will obviously include several consecutive and parallel dissociation and reaction steps. Also, we emphasize that by $HC$ we do not mean simply the adsorbed parent alkane or alkyl, but any $CH_x$ fragment between the alkyl and carbon. Nevertheless, our model should allow a qualitative test of the previously cited hypothesis.

The key point of the model is site competition between the hydrocarbon and oxygen on the catalyst surface. Competitive, nondissociative adsorption and first-order LH reaction for the preceding mechanism yields the well-known catalytic rate law:

$$r = k_R \frac{K_H K_{O_2} P_{HC} P_{O_2}}{(1 + K_{HC} P_{HC} + K_{O_2} P_{O_2})^2} \tag{2}$$

where $k_R$ denotes the reaction rate constant of the overall reaction, $K_i$ is the adsorption–desorption equilibrium constants, and $P_i$ the partial pressures. The index $HC$ refers to the respective hydrocarbons. Since at this point we are only interested in modeling the ignition curve, we have also assumed that the coverages of both the fuel and oxygen are determined by the adsorption–desorption equilibrium. (Obviously, this assumption, as well as the neglection of mass transport limitations, is only valid for negligible surface reaction, and thus will break down upon ignition.)

Both $k_R$ and $K_i$ are assumed to be functions of temperature following the usual Arrhenius-type dependency:

$$k_R = k_{R,0} \exp\left\{-\frac{E_R}{RT}\right\}$$

and

$$K_i = K_{i,0} \exp\left\{-\frac{\Delta H_{\mathrm{ad},i}}{RT}\right\},$$

with $E_R$ denoting the apparent activation energy of the surface reaction (RIII) and $\Delta H_{\mathrm{ad},i}$ the heats of adsorption of the reactants. Taking into consideration the hypothesis of larger sticking coefficient for oxygen on the catalyst, that is, a mostly oxygen-covered catalyst surface up to ignition, we now assume $K_{O_2} P_{O_2} \gg (1 + K_{HC} P_{HC})$. This yields the simplified rate expression:

$$r \cong k_R \frac{K_{HC}}{K_{O_2}} \frac{P_{HC}}{P_{O_2}} = k_0 \frac{K_{HC,0}}{K_{O_2,0}} \exp\left\{-\frac{E_{\mathrm{app}}}{RT}\right\} \Phi, \qquad (3)$$

where $E_{\mathrm{app}} = E_R + \Delta H_{\mathrm{ad},HC} - \Delta H_{\mathrm{ad,O_2}}$ denotes the apparent activation energy for the overall reaction. Thus, we obtain a rate expression that is directly proportional to the ratio of the partial pressure of the alkane to the oxygen partial pressure, that is the (conventional) equivalence ratio $\Phi$. This is in qualitative agreement with the results of an analysis by Harold et al. (1987) for ethane oxidation on Pt, yielding a cubic dependence of the kinetic rate law on the ethane partial pressure and an inverse cubic dependence on the oxygen partial pressure (Harold and Luss, 1985).

Following our definition of ignition as the turning point of the $T(VI)$ curve (the point where the plot of foil temperature vs. power input has a vertical slope), the ignition criterion is (cf. Figure 1c):

$$\left|\frac{\partial (VI)}{\partial T}\right|_{\Phi} = \alpha + \left|\frac{\partial r}{\partial T}\right|_{\Phi} \Delta H_R = 0 \qquad (4)$$

where $\Phi$ is defined as $p_{HC}/p_{O_2}$, and we have neglected the temperature dependence of $\Delta H_R$. Substituting the simplified rate expression (Eq. 3) into Eq. 4, finally yields (after transformation into the modified equivalence ratio $\Theta$),

$$\Theta(T) = \left[1 - \frac{a}{T^2} \exp\left\{-\frac{E_{\mathrm{app}}}{RT}\right\}\right]^{-1}. \qquad (5)$$

This function has two adjustable parameters, an apparent activation energy $E_{\mathrm{app}}$ and a preexponential parameter $a$ that is a lumping of thermodynamic, geometrical, and kinetic factors. They can be fitted for $0.2 < \Theta < 0.75$ with high confidence for all four alkanes, yielding apparent activation energies that drop with increasing carbon number from $E_{\mathrm{app}} \approx 110$ kJ/mol for methane and $E_{\mathrm{app}} \approx 95$ kJ/mol for ethane to $E_{\mathrm{app}} \approx 80$ kJ/mol for propane and isobutane. The lumped preexponential parameter $a$ varies between values of about $-5 \times 10^{11}$ K$^2$ and $-5 \times 10^{13}$ K$^2$, the negative sign being consistent with the fact that this parameter contains the heat of reaction $\Delta H_R$ of the surface reaction step (RIII), which must be negative for a typical exothermic oxidation reaction.

The fact that the calculated energies of $\approx 80$–110 kJ/mol are reasonable values for these overall activation energies of surface reactions together with the good fit between the calculated function $\Theta(T)$ and the experimental data (cf. Figure 8), and finally the observation that the calculated activation energies drop with increasing carbon number, can be taken as evidence that the observed dependence of the ignition temperature vs. equivalence ratio can be explained by the different adsorption properties of the hydrocarbons vs. oxygen.

### *Simple model: Olefins*

The surface ignition of the olefins clearly does not fit the same trend as the ignition of the alkanes. Not only does ignition occur at considerably higher surface temperatures and lower fuel/air ratios than for the corresponding alkanes, but in particular the ignition temperatures *increase* with an increasing equivalent ratio. This behavior, which is *opposite* to the behavior observed during alkane ignition, can thus be taken as an indication that ethylene and propylene have much higher sticking coefficients than both the alkanes and oxygen.

We thus set up a similar model as the one for alkane ignition under the opposite assumption of a mainly hydrocarbon-covered surface. This derivation (which will not be given in detail here) yields

$$r \cong k_R \frac{K_{O_2}}{K_{HC}} \frac{P_{O_2}}{P_{HC}} = k_0 \frac{K_{O_2,0}}{K_{HC,0}} \exp\left\{-\frac{E^*_{\mathrm{app}}}{RT}\right\} \frac{1}{\Phi}, \qquad (6)$$

and from there

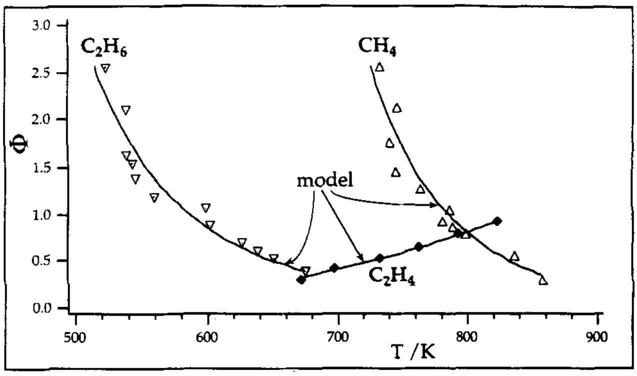

**Figure 8. Examples of model-fit curves and experimental data points for methane, ethane, and ethylene.**

Note that this graph depicts the "conventional" equivalence ratio $F$ vs. absolute temperature. A two-parameter fit reproduces the correct curvature.

$$\Theta(T) = \left[1 - bT^2 \exp\left\{-\frac{E^*_{\rm app}}{RT}\right\}\right]^{-1}, \qquad (7)$$

with $E_{\rm app} = E_R - \Delta H_{{\rm ad},HC} + \Delta H_{{\rm ad,O}_2}$ and $b$ again lumping the model constants. Obviously, this expression gives the qualitatively opposite dependence of $\Theta(T)$ (which might be more easily seen by comparing the dependencies of $r(\Phi)$ in the rate equations 6 and 3). A corresponding fit to expression (7) (cf. Figure 8) yields apparent activation energies of $E_{\rm app} \approx 47$ kJ/mol for ethylene and $E_{\rm app} \approx 35$ kJ/mol for propylene (preexponential parameter $b \approx -7 \times 10^7$ $K^2$ and $-6 \times 10^8$ $K^2$, respectively).

The same line of reasoning can be applied to the minima in the surface-ignition curves for both the alkanes and the olefins. Since the assumption of hydrocarbon-covered or oxygen-covered surfaces obviously will have to break down at extreme values of the equivalence ratio, the minima in ignition temperature for very large equivalence ratios in the case of alkane oxidation and very small equivalence ratios in the case of olefin oxidation can be taken to indicate the crossing from one limiting case to the other (with increasing equivalence ratio from a largely oxygen-covered to a hydrocarbon-covered surface). Following this reasoning, the lack of a local minimum ignition temperature for methane should indicate that this hydrocarbon has such a low sticking probability that this crossing will occur very close to the boundary of surface flammability and is therefore no longer observable in the experiment.

Although not much experimental data on heats of adsorption for hydrocarbons on Pt are available in the literature, we attempted some further interpretation of these results. Theoretical bond-order-conservation (BOC) calculations by Shustorovich and Bell yield heats of adsorption of $-25$ kJ/mol and $-20$ kJ/mol for methane and ethane and $-50$ kJ/mol for ethylene on Pt(111) (Bell, 1991). Using these values and a value of $-213$ kJ/mol ($-51$ kcal/mol) as heat of adsorption of oxygen on Pt (Campbell et al., 1981), we can obtain estimates for the activation energies for the surface-reaction step (RIII) from the previously calculated apparent activation energies for the alkanes and olefins (keeping in mind that this surface-reaction step (RIII) itself lumps a complex surface chemistry into one overall step). These estimates yield activation energies of about 200 kJ/mol in the case of ethylene oxidation and about $-95$ kJ/mol for methane and ethane oxidation. While the value of 200 kJ/mol seems reasonable (though somewhat high), the negative number in the case of the alkanes is clearly unphysical. Yet, since in this case we are concerned with a mainly oxygen-covered surface, the heat of adsorption of $-213$ kJ/mol for oxygen that has been determined under low-coverage UHV conditions is probably far too high. Thus, our simple model yields consistent results, although unfortunately too little information on the detailed chemistry of these oxidation reactions is available to allow a further interpretation of these values.

We conclude that the ignition behavior of the hydrocarbons studied in this investigation can be explained quite well in terms of site competition between the fuel and oxygen, where for alkanes behavior over a wide range of fuel/air ratios is dominated by an oxygen-covered catalyst, while for the olefins a hydrocarbon overlayer seems to dominate the ignition behavior.

### *Surface extinction*

The extinction temperatures essentially show the same trend toward decreasing temperatures with increasing chain length as did the ignition temperatures for the alkanes. This can be taken as an indication that the C—H bond strength is an important factor not only during lightoff of the surface reactions, but also plays a major role during stationary reaction conditions at comparatively low surface temperatures.

Furthermore, the extinction temperatures on the fuel-rich side of the bifurcation diagram for all four hydrocarbons lie below those in the fuel-lean regime. This can be explained by the different reaction paths with different heats of reaction under fuel-lean and fuel-rich conditions. For very fuel-lean mixtures the reaction rate for total oxidation will be enhanced compared to that of the partial oxidation reactions, since the higher activation energy for this reaction path on the catalyst is (over)compensated by high oxygen coverage, resulting in a higher overall reaction rate. Since extinction occurs when the net adsorption rate exceeds the surface reaction rate, and thus poisons the surface by inhibiting further dissociation of molecular adsorbates (assuming that desorption of products is always a very fast step), by comparing the fuel-rich and fuel-lean parts of the extinction curves, one essentially examines reaction channels with comparable rates but very different heats of reaction. Therefore, it is obvious that the extinction temperatures for fuel-lean mixtures (the highly exothermic total oxidation reactions) will lie higher than for fuel-rich mixtures.

The decrease of the extinction temperatures as one approaches the "surface flammability limits" both at extremely fuel-rich and fuel-lean mixtures, is unexpected. One would expect that toward these extremes, the surface is much more likely to be poisoned by unreacted adsorbates of the highly overstoichiometric reactant. Therefore, extinction should occur at increasingly high temperatures as one approaches the limits of surface flammability. Instead, the experimental data show the exact opposite trend. While this can be rationalized in terms of the bifurcation behavior of these systems with the need for closing the loop between surface ignition and surface extinction, so far we have no consistent explanation for this behavior in terms of the surface-reaction mechanism.

### *Autothermal behavior*

The autothermal behavior of the reactions allows qualitative conclusions about the main reaction paths on the particular catalyst surface: Following the argument used during the discussion of the extinction curves, the heat-production term under stationary conditions is determined by the reaction rate for a particular reaction path and the corresponding heat of reaction. Therefore, one expects the autothermal curve to show a maximum where the heat evolution exhibits a maximum. From the fact that the autothermal temperatures for the alkanes peak at or near the stoichiometric composition for partial oxidation to CO and $H_2O$, one can conclude that Pt is actually a good catalyst for partial oxidation, though not for the formation of syngas or olefins from hydrocarbons. This agrees well with earlier observations in our group, that Rh is a much better catalyst for syngas formation than Pt (Hickman and Schmidt, 1992, 1993a,b). Furthermore, it appears from the much less pronounced maximum in the case of ethane, that the Pt catalyzed reaction is less selective toward CO and $H_2O$ for this alkane. Again, this compares well with previous experiments that showed that during ethane oxidation over a Pt monolith a very high yield of ethylene could be obtained (Huff and Schmidt, 1993; Huff et al., 1994). Yet, this is obviously only a rough and qualitative indicator for the selectivity of the catalytic oxidation reactions. Nevertheless, the simplicity of the experimental setup and procedure make it a very fast and simple way to do laboratory screening of potential partial oxidation catalysts.

So far we have considered ignition, extinction, and autothermal behavior of the surface reaction separately. If one combines these three surface reaction branches of the bifurcation diagram, they form an isola of "inaccessible" states, that is, of surface temperatures, for which no stationary state of the catalytic surface reaction exists (cf. Figure 2). For all hydrocarbons studied in this investigation, these temperature ranges continuously widen as one moves away from the boundaries of surface flammability toward the peak autothermal temperatures. This is certainly an undesirable feature for practical purposes, since it not only limits the capability of "tuning" the reaction toward such desired properties as reaction selectivity by reducing the accessible parameter space, but also calls for good process control, since comparatively small changes in composition or temperature could cause the reaction to extinguish.

### *Homogeneous ignition*

The branches for the gas-phase ignition temperatures of the hydrocarbons do not show many similarities between the different fuels. Particularly, the extremely high and sharply peaked ignition temperatures for methane/air mixtures differ greatly from the other fuels. This peculiar behavior of methane/air and natural gas/air mixtures has been observed before. As early as 1927, Coward and Guest observed a maximum in the ignition temperature near the stoichiometric composition for total oxidation for the combustion of natural gas over platinum (Coward and Guest, 1927), which they explained by reactant depletion near the catalyst surface due to the surface reaction. This effect has since been proven to exist in a simplified mathematical model by Liñán and Williams (1981). Using an asymptotic analysis of a model incorporating a general homogeneous and heterogeneous reaction term, they demonstrated that a catalytic reaction can effectively suppress homogeneous ignition if the surface reaction is sufficiently fast. These results are consistent with the observed behavior of methane/air mixtures in our experiments.

However, in another study, Griffin and Pfefferle, who had also observed a maximum temperature during homogeneous ignition of methane/air mixtures over a catalytic Pt surface, contradict these explanations, claiming that observed maximum is actually only an artifact of the experimental procedure (Griffin and Pfefferle, 1990). They proved the validity of their explanation for their experiments, which did not allow for a clear separation between heterogeneous and homogeneous ignition without further dilution of the gas phase, since upon ignition of the surface reaction the temperature of their catalytic wires shot up high enough to ignite the homogeneous gas-phase reaction. Unfortunately, they do not report in detail how they determined the homogeneous ignition temperatures under these conditions, so we can only speculate about the reason for their observation and why it did not occur in our experiments.

In any case, their reasoning does not apply to our experiments, since in our case the homogeneous ignition of the gas phase was always well separated from the ingition of the surface reaction, that is, for any composition of the gas phase we found stationary states in which only the surface reaction was ignited. Also, we can eliminate influences by an ignition delay of the homogeneous gas-phase reaction, since typically delay times for gas-phase ignition are of the order of seconds or well below, while by our criterion for a stationary state, we waited for at least one minute before accepting a data point as stationary. Finally, we never observed any transient overshoot of the catalyst temperature during ignition of the surface reaction, as seems to have been the case in the experiments of Griffin and Pfefferle. (This can be easily explained by the fact that they were using a platinum wire with the same thickness as our Pt foil (250 $\mu$m). Since the transient peak temperature will be proportional to the ratio of heat evolved in the surface reaction and heat absorbed by the catalyst volume, and thus by the ratio of surface to volume of the catalyst, which is about twice as large for a wire than for a foil with the same thickness, it is apparent that one has to expect considerably higher transients in the case of catalytic wires.)

Thus, we are positive that the maximum in the gas-phase ignition temperature is not an experimental artifact in our case. We conclude, that it actually has to be explained by reactant depletion in the boundary layer above the catalytic surface. In addition, separate experiments with different foils and varying flow rates reproduced the results within experimental errors, indicating that the homogeneous ignition temperatures do not depend sensitively on the specific characteristics of the local flow field (on a particular set of boundary-layer–surface conditions).

The lack of a maximum ignition temperature in the case of ethane/air and isobutane/air mixtures could be due to the fact that these mixtures ignite at considerably lower temperatures than methane ($\approx$ 950–1,200°C vs. 1,200–1,500°C). As Liñán and Williams demonstrated in their analysis, this suppression of homogeneous ignition requires a high enough surface reaction rate (Liñán and Williams, 1981). Thus, the lower ignition temperatures of the higher hydrocarbons could lower the surface reaction rate down to a point where it is no longer capable of suppressing gas-phase ignition.

Finally, for propane/air mixtures the ignition temperatures display a peculiar trend, exhibiting a minimum ignition temperature at an equivalence ratio of about 0.42 and a maximum at 0.6. This behavior can be explained by a superposition of the two effects mentioned earlier: on the fuel-lean side, a "weak" surface reaction does not appreciably influence gas-phase ignition, and therefore an increasing trend as for ethane and isobutane is observed. On the fuel-rich side, a very fast surface reaction leads to a boundary-layer depletion as observed for methane/air mixtures, and therefore to a similar maximum in gas-phase ignition temperatures. This interpretation is justified by the observation of the extremely strongly peaked autothermal temperatures for propane, where the steep rise from about 500°C at the limits of autothermal behavior to about 1,000°C at the maximum indi-

**Table 2. Comparison of Published Flammability Limits for Hydrocarbon/Air Mixtures with Our Experimental Data for Homogeneous Flammability over Pt Foils**

| | Lean (Publ.) | Rich (Publ.) | Lean (Exp.) | Rich (Exp.) |
|---|---|---|---|---|
| Methane | 0.33 | 0.6 | 0.35 | 0.6 |
| Ethane | 0.34 | 0.69 | 0.36 | 0.69 |
| Propane | 0.35 | 0.70 | 0.35 | 0.66 |
| Isobutane | 0.37 | 0.73 | 0.36 | 0.72 |
| Ethylene | 0.29 | 0.81 | 0.44 | — |
| Propylene | 0.31 | 0.71 | 0.38 | — |

Source: Lewis and von Elbe (1987).

cates a large increase in reaction rate over this range. Since the maximum in autothermal temperature coincides with the maximum in gas-phase ignition, the preceding interpretation is consistent with both our interpretation of the autothermal and the gas phase ignition branches for all hydrocarbons.

Comparing our measured homogeneous flammability limits with published data for the flammability of hydrocarbon/air mixtures shows a very good agreement between these values for the four alkanes (Table 2). Taking into account the accuracy and step size in our experiments, the agreement of 0.02 and less for all four alkanes studied has to be taken as almost perfect. This agreement between our values, obtained by igniting the gas mixture through the heat of the catalytic foil, and the data in the literature for homogeneous ignition that is typically obtained by spark ignition, indicates that the catalytic surface does not influence the ignitability of the mixtures very near the homogeneous flammability limits. Otherwise one should observe a narrowing of the region of flammability, since the surface reaction should make a lean gas mixture even leaner and a rich mixture richer, thus tending to move the composition in the boundary layer out of the flammability limits. This effect has also been shown in a simple general mathematical model by Law and Chung (1983). Again, this effect will depend on the degree of depletion in the boundary layer and will only be seen for surface reactions that are fast enough.

The picture looks very different for olefin oxidation. Unfortunately, as explained in the experimental section, we were only able to determine the fuel-lean half of the bifurcation diagrams for the olefins. Yet, this part shows a noticeable disagreement between the published gas-phase flammability limits and our experimental results. This considerably higher fuel-lean limit of the gas-phase flammability region for ignition over the catalytic Pt foil as compared to truly homogeneous ignition indicates that the surface reaction is actually strongly influencing the gas-phase ignition in this case. Since mass transfer rates are comparable for alkane and olefin oxidation, one can conclude from these observations that the high-temperature surface reaction has to be considerably faster for the olefin oxidation than for alkane oxidation. This is again consistent with the observation that at lower temperatures olefins are considerably more reactive than the corresponding alkanes, as indicated by their markedly lower fuel-lean limit for surface flammability.

Finally, comparing the gas-phase flammability limits with the catalytic surface flammabilities, one immediately recognizes the far larger width of the region of surface flammability. This, of course, is the reason for the use of catalytically stabilized burners in combustion, since the combustion process thus becomes not only much less sensitive to fluctuations and changes of the feed composition, but also allows for a much leaner (and therefore much more economical) operation of commercial burners.

### *Carbon*

A very remarkable feature in these experiments is the fact that under no conditions did we find any evidence for multilayer carbon formation on the catalyst surface during the oxidation of the saturated hydrocarbons. No time-dependent deactivation of the catalyst was observed under any experimental conditions. Also, even for the most fuel-rich mixtures and highest temperatures, no visual coke formation occurred either on the catalyst surface or at any other point in the reactor. Finally, the results were always and under all conditions reproducible within experimental accuracy, independent of the catalyst "history," that is, on previous experiments with the same catalytic foil. These observations are a strong indication that no poisoning of the catalyst surface by any carbonaceous deposits took place. This is surprising, since at high enough temperatures and at a fuel content beyond stoichiometric, carbon formation is thermodynamically strongly favored. Yet, the observed lack of carbon formation coincides well with similar observations in this laboratory during the partial oxidation of hydrocarbons on monolithic Pt catalysts, where no evidence for coking had been found (Huff et al., 1994; Schmidt and Huff, 1994). Since in these experiments virtually all the reaction takes place within milliseconds (within about the first millimeter of the monolithic catalyst), the catalytic foil in our stagnation-point setup can be taken as a simple approximation of those experiments. It is therefore consistent with those results that we do not observe carbon formation, although at this point we are not able to explain this observation.

In contrast to that, carbon poisoning seemed to take place during the oxidation of the unsaturated hydrocarbons under fuel-rich conditions, as indicated by the lack of any observable surface reaction in these cases. Futhermore, the remarkable observation that the ignition temperatures for the olefins lie considerably *above* those of the corresponding alkanes can be taken as an indication that some carbon poisoning of the catalyst surface is taking place even under fuel-lean conditions where a surface reaction was observed, exactly as predicted by our simple model for surface ignition.

This again can be taken as an indication that olefins are much more reactive than alkanes on Pt, though this in fact inhibits oxidation reactions. Olefins seem to undergo rapid C—C bond scission, which then leads to the formation of carbonaceous deposits that poison the catalytic surface for oxygen adsorption. This is also consistent with the assumption of a mainly hydrocarbon-covered surface during the ignition of the surface reaction for equivalence ratios larger than about 0.2. So again we obtain a consistent picture between the different branches of the bifurcation diagrams.

## Summary

The intent of this investigation was to obtain consistent data for the ignition/extinction behavior of hydrocarbons during catalytic oxidation over noble metal catalysts. We have produced complete bifurcation diagrams for methane, ethane, propane, and isobutane as well as ethylene and propylene/air mixtures over a Pt foil catalyst at atmospheric pressure for room temperature gases.

These diagrams showed a clear distinction between the behavior of the saturated hydrocarbons and the unsaturated hydrocarbons. While the alkane/air mixtures show a decreasing ignition temperature with increasing equivalence ratio up to a minimum ignition temperature near the fuel-rich surface flammability limit, the olefins ignite at much leaner mixtures and display their minimum ignition temperature well into the fuel-lean side of the bifurcation diagram.

These observations could be explained and modeled in terms of different adsorption properties of the alkanes, olefins, and oxygen on the Pt surface, suggesting that during alkane oxidation the reaction takes place on a mainly oxygen-covered surface, while during olefin oxidation the surface seems to be covered by a hydrocarbon overlayer. The fact that a very simple model for surface ignition of these hydrocarbons works so well suggests a need for accurate surface science investigations of these reaction systems, the results of which should allow one to develop quantitative models applicable to engineering situations.

The homgeneous gas-phase ignition over the catalytic foil was found to depend strongly on the rate of the surface reaction. We could distinguish between methane/air mixtures, which displayed a strong maximum in gas-phase ignition temperatures due to boundary-layer depletion, and ethane and isobutane/air mixtures, which did not show a similar effect. Propane/air mixtures take an intermediate position, showing both types of behavior, depending on the fuel/air ratio.

An interesting aspect of these studies was the observation that under no conditions was coke formation observed during the oxidation of the alkanes. The fact that fuel-rich olefin/air mixtures have much higher ignition temperatures on the Pt surface indicated strong carbon poisoning for these fuels.

We are currently extending these studies onto different noble metal catalysts to examine the influence of metal surface chemistry on these phenomena.

## Acknowledgment

This research was supported by DOE grant DE-FG02-88ER13878-AO2 and by a Feodor-Lynen fellowship of the Alexander von Humboldt-Foundation (G.V.).

## Literature Cited

Ablow, C. M., S. Schechter, and H. Wise, "Catalytic Combustion in a Stagnation Point Boundary Layer," *Combust. Sci. Tech.*, **22**, 107 (1980).

Bell, A. T., "Relationship of Reaction Energetics to the Mechanism and Kinetics of Heterogeneously Catalysed Reactions," *Metal Surface Reaction Energetics*, E. Shustorovich, ed., Verlag Chemie, Weinheim, p. 191 (1991).

Benson, S. W., "Bond Energies," *J. Chem. Educ.*, **42**, 502 (1965).

Campbell, C. T., G. Ertl, H. Kuipers, and J. Segner, "A Molecular Beam Study of the Adsorption and Desorption of Oxygen from a Pt(111) Surface," *Surf. Sci.*, **107**, 220 (1981).

Cattolica, R. J., and R. W. Schefer, "The Effect of Surface Chemistry on the Development of the [OH] in a Combustion Boundary Layer," *Proc. 19th Symp. (Int.) on Combustion*, p. 311 (1982).

Cho, P., and C. K. Law, "Catalytic Ignition of Fuel/Oxygen/Nitrogen Mixtures over Platinum," *Combust. Flame*, **66**, 159 (1986).

Coward, H. F., and P. G. Guest, "Ignition of Natural Gas-Air Mixtures by Heated Metal Bars," *J. Amer. Chem. Soc.*, **49**, 2479 (1927).

Frank-Kamenetskii, D. A., *Diffusion and Heat Transfer in Chemical Kinetics*, Academic Press, New York (1969).

Germain, J. E., *Catalytic Conversion of Hydrocarbons*, Academic Press, London (1969).

Griffin, T., and L. D. Pfefferle, "Gas Phase and Catalytic Ignition of Methane and Ethane in Air over Platinum," *AIChE J.*, **36**, 861 (1990).

Griffin, T. A., L. D. Pfefferle, M. J. Dyer, and D. R. Crosley, "The Ignition of Methane/Ethane Boundary Layer Flows by Heated Catalytic Surfaces, *Combust. Sci. Tech.*, **65**, 19 (1989).

Harold, M. P., and D. Luss, "An Experimental Study of Steady-State Multiplicity Features of Two Parallel Catalytic Reactions," *Chem. Eng. Sci.*, **40**, 39 (1985).

Harold, M. P., and D. Luss, "Use of Bifurcation Map for Kinetic Parameter Estimation. 1. Ethane Oxidation," *Ind. Eng. Chem. Res.*, **26**, 2092 (1987).

Harold, M. P., M. Sheintuch, and L. Luss, "Analysis and Modeling of Multiplicity Features," *Ind. Eng. Chem. Res.*, **26**, 786 (1987).

Hiam, L., H. Wise, and S. Chaikin, "Catalytic Oxidation of Hydrocarbons on Platinum," *J. Catal.*, **9**, 272 (1968).

Hickman, D. A., and L. D. Schmidt, "Synthesis Gas Formation by Direct Oxidation of Methane over Pt Monoliths," *J. Catal.*, **138**, 267 (1992).

Hickman, D. A., and L. D. Schmidt, "Production of Syngas by Direct Catalytic Oxidation of Methane," *Science*, **259**, 343 (1993a).

Hickman, D. A., and L. D. Schmidt, "Steps in CH4 Oxidation on Pt and Rh Surfaces: High-Temperature Reactor Simulations," *AIChE J.*, **39**, 1164 (1993b).

Huff, M., and L. D. Schmidt, "Ethylene Formation by Oxidative Dehydrogenation of Ethane over Monoliths at Very Short Contact Times," *J. Phys. Chem.*, **97**, 11815 (1993).

Huff, M., P. M. Torniainen, and L. D. Schmidt, "Partial Oxidation of Alkanes over Nobel Metal Coated Monoliths," *Catal. Today*, **21**, 113 (1994).

Law, C. K., and S. H. Chung, "Thermal and Catalytic Inhibition of Ignition through Reactant Depletion," *Combust. Sci. Technol.*, **32**, 307 (1983).

Lewis, B., and G. von Elbe, *Combustion, Flames and Explosions of Gases*, Academic Press, New York (1987).

Liñán, A., and F. A. Williams, "Note on Ignition by a Hot Catalytic Surface," *SIAM J. Appl. Math.*, **40**, 261 (1981).

Liñán, A., and F. A. Williams, *Fundamental Aspects of Combustion*, Oxford Engineering Science Series, Oxford Univ. Press, Oxford, (1993).

Lunsford, J. H., "The Role of Surface-Generated Gas-Phase Radicals in Catalysis," *Langmuir*, **5**, 12 (1989).

McMaster, M. C., C. R. Arumainayagam, and R. J. Madix, "Molecular Propane Adsorption Dynamics on Pt(111)," *Chem. Phys.*, **177**, 461 (1993).

McMaster, M. C., and R. J. Madix, "Alkane Dissociation Dynamics on Pt(100)$-(1\times 2)$," *J. Chem. Phys.*, **98**, (1993).

Patterson, W. R., and C. Kemball, The Catalytic Oxidation of Olefins aon Metal Films," *J. Catal.*, **2**, 465 (1963).

Pfefferle, L. D., and W. C. Pfefferle, "Catalysis in Combustion,"*Catal. Rev.-Sci. Eng.*, **29**, 219 (1987).

Satterfield, C. N., *Heterogeneous Catalysis in Industrial Practice*, McGraw-Hill, New York (1991).

Schmidt, L. D., and M. Huff, "Partial Oxidation of CH4 and C2H6 over Noble Metal-Coated Monoliths," *Catal. Today*, **21**, 443 (1994).

Schwartz, A., L. L. Holbrook, and H. Wise, "Catalytic Oxidation Studies with Platinum and Palladium," *J. Catal.*, **21**, 199 (1971).

Szuromi, P. D., J. R. Engstrom, and W. H. Weinberg, "Adsorption and Reaction of *n*-Alkanes on the Pt(110)$-(1\times 2)$ Surface," *J. Phys. Chem.*, **89**, 2497 (1985).

Thomas, D. J., R. Willi, and A. Baiker, "Partial Oxidation of Methane: The Role of Surface Reactions," *Ind. Eng. Chem. Res.*, **31**, 2272 (1992).

Trimm, D. L., "Catalytic Combustion," *Appl. Catal.*, **7**, 249 (1983).

Williams, W. R., M. T. Stenzel, X. Song, and L. D. Schmidt, "Bifurcation Behaviour in Homogeneous-Heterogeneous Combustion: I. Experimental Results over Platinum," *Combust. Flame*, **84**, 277 (1991).

*Manuscript received Apr. 12, 1995, and revision received July 10, 1995.*